

## Size-Tunable Emission from 1,3-Diphenyl-5-(2-anthryl)-2-pyrazoline Nanoparticles

Debao Xiao,<sup>†</sup> Lu Xi,<sup>†</sup> Wensheng Yang,<sup>†</sup> Hongbing Fu,<sup>†</sup> Zhigang Shuai,<sup>†</sup>  
Yan Fang,<sup>‡</sup> and Jiannian Yao<sup>\*†</sup>

*Contribution from the Key Laboratory of Photochemistry and Laboratory of Organic Solids,  
Center for Molecular Science, Institute of Chemistry, Chinese Academy of Sciences,  
Beijing 100080, P. R. China*

Received September 24, 2002; Revised Manuscript Received April 2, 2003; E-mail: jnyao@mail.iccas.ac.cn

**Abstract:** Organic nanoparticles of 1,3-diphenyl-5-(2-anthryl)-2-pyrazoline (DAP) ranging in average diameters from 40 to 160 nm were prepared through the reprecipitation method. The average diameters of the particles were controlled by variation of the aging time. We found that DAP nanoparticles exhibit the size-dependent optical properties. The absorption transitions of the nanoparticles at the lower-energy side experience a bathochromic shift with an increase in the particle size as a result of the increased intermolecular interactions, while the higher-energy bands of anthracene split possibly due to the electronic coupling between the pyrazoline ring of one molecule and the anthracene moiety of the neighboring molecule. Most interestingly, the nanoparticle emission in the blue light region from pyrazoline chromophore shifts to shorter wavelengths with an increase in the particle size, accompanied with a relatively gradual dominance of the emission at about 540 nm from an exciplex between the pyrazoline ring of one molecule and the anthracene moiety of the neighboring molecule. The hypsochromic shift in the emission of DAP nanoparticles was identified as originating from the pronounced decrease in the Stokes shift due to the restraint of vibronic relaxation and the configuration reorganization induced by the increased intermolecular interaction.

### Introduction

Organic materials used as light-emitting candidates have attracted tremendous research activities in the development of novel optoelectronic devices and full color flat panel displays due to their advantages such as high luminescence efficiencies.<sup>1</sup> The colors that they emit are usually tailored either by chemical modification of their structures or by doping treatment.<sup>2</sup> It is known that, similar to inorganic ones,<sup>1–10</sup> nanoparticles from organic molecules also show the size-dependent optical absorption,<sup>11–15</sup> which may not originate from the so-called

quantum confinement because of the small radii of the Frenkel exciton. In organic molecular crystals, the electronic properties are fundamentally different from those of inorganic metals and semiconductors because of the weak intermolecular interaction force of the van der Waals type or the hydrogen bond.<sup>16</sup> The change in the absorption transition of organic nanoparticles as a function of particle size may arise from the aggregate effect,<sup>13,15</sup> surface effect,<sup>15</sup> or the increased intermolecular interaction induced by the change of lattice.<sup>11,12</sup>

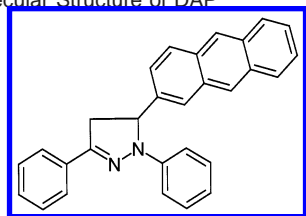
Recently, a study has been reported on the changes in the emission spectra of organic nanoparticles.<sup>12,15,17</sup> For example, perylene nanoparticles were found to exhibit size-dependent emission<sup>12</sup> because of the reduction of the barrier from S-exciton to F-exciton states in the nanoparticles. In light of the fact that pyrazoline derivatives have been widely used as optical brightening agents for textiles and paper because of their strong fluorescence<sup>18,19</sup> and as the hole-conducting medium in photoconductive materials<sup>20,21</sup> and electroluminescence (EL) devices, our group has investigated the size-dependent optical properties of the nanoparticles from a series of pyrazoline compounds.

<sup>†</sup> Key Laboratory of Photochemistry.

<sup>‡</sup> Laboratory of Organic Solids.

- (1) Forrest, S. *MRS Bull.* **2001**, *26*, No. 2, 108–112.
- (2) Tang, C. W.; VanSlyke, S. A.; Chen, C. H. *J. Appl. Phys.* **1989**, *65*.
- (3) Alivisatos, A. P. *Science* **1996**, *271*, 933.
- (4) Peng, X. G.; Schlamp, M. C.; Kadavanich, A. V.; Alivisatos, A. P. *J. Am. Chem. Soc.* **1997**, *119*, 7019–7029.
- (5) Peng, X. G.; Manna, L.; Yang, W. D.; Wickham, J.; Scher, E.; Kadavanich, A.; Alivisatos, A. P. *Nature* **2000**, *404*, 59.
- (6) Schlamp, M. C.; Peng, X. G.; Alivisatos, A. P. *J. Appl. Phys.* **1997**, *82*, 5837–5842.
- (7) Bruchez, M.; Moronne, M.; Gin, P.; Weiss, S.; Alivisatos, A. P. *Science* **1998**, *281*, 2013–2016.
- (8) Chan, W. C. W.; Nie, S. M. *Science* **1998**, *281*, 2016–2018.
- (9) Lieber, C. M. *Solid State Commun.* **1998**, *107*, 607–616.
- (10) Smalley, R. E.; Yakobson, B. I. *Solid State Commun.* **1998**, *107*, 597–606.
- (11) Kasai, H.; Kamatani, H.; Okada, S.; Oikawa, H.; Matsuda, H.; Nakanishi, H. *Jpn. J. Appl. Phys.* **1996**, *35*, L221.
- (12) Kasai, H.; Kamatani, H.; Yoshikawa, Y.; Okada, S.; Oikawa, H.; Watanabe, A.; Itoh, O.; Nakanishi, H. *Chem. Lett.* **1997**, 1181.
- (13) Fu, H. B.; Yao, J. N. *J. Am. Chem. Soc.* **2001**, *123*, 1434–1439.
- (14) Forrest, S. R. *Chem. Rev.* **1997**, *97*, 1793–1896.
- (15) Fu, H. B.; Loo, B. H.; Xiao, D. B.; Xie, R. M.; Ji, X. H.; Yao, J. N.; Zhang, B. W.; Zhang, L. Q. *Angew. Chem., Int. Ed.* **2002**, *41*, 962–965.

- (16) Silinsh, E. A. *Organic Molecular Crystals: Their Electronic States*; Springer-Verlag: Berlin, 1980.
- (17) Seko, T.; Ogura, K.; Kawakami, Y.; Sugino, H.; Toyotama, H.; Tanaka, J. *Chem. Phys. Lett.* **1998**, *291*, 438–444.
- (18) Sandler, S. R.; Tsou, K. C. *J. Chem. Phys.* **1963**, *39*, 1062.
- (19) Borsenberger, P. M.; Schein, L. B. *J. Phys. Chem.* **1994**, *98*, 233.
- (20) Melz, P. J.; Champ, R. B.; Chang, L. S.; Chiou, C.; Keller, G. S.; Liclican, L. C.; Neiman, R. R.; Schattuck, M. D.; Weiche, W. J. *Photogr. Sci. Eng.* **1977**, *21*, 73.
- (21) Gao, X. C.; Cao, H.; Zhang, L. Q.; Zhang, B. W.; Cao, Y.; Huang, C. H. *J. Mater. Chem.* **1999**, *9*, 1077–1080.

**Scheme 1.** Molecular Structure of DAP

We found that the formation of aggregates also influences the size-dependent optical properties of 1-phenyl-3-((dimethylamino)styryl)-5-((dimethylamino)phenyl)-2-pyrazoline (PDDP) nanoparticles,<sup>13</sup> in addition to previous opinions about the change of the lattice state. Furthermore, the multiple emissions from alternate derivative 1,3-diphenyl-5-pyrenyl-2-pyrazoline (DPP) nanoparticles<sup>15</sup> were observed, the emission color from which can be tuned either by the particle size or by the excitation wavelength.

The presentation is an extension of the above-mentioned research interest. In this paper, 1,3-diphenyl-5-(2-anthryl)-2-pyrazoline (DAP) was employed as a model compound to fabricate its corresponding nanoparticles by the reprecipitation method. The as-prepared DAP nanoparticles were observed to exhibit the size-dependent bathochromic absorption transition induced by the increased intermolecular interaction, accompanied by the split band of the higher-energy band of anthracene possibly caused by the electronic coupling between the molecules. The emission of the pyrazoline chromophore was blue-shifted with an increase in the particle size arising from the reduced Stokes shift due to the restraint of vibronic relaxation and the configuration reorganization induced by the increased intermolecular interaction. Furthermore, an exciplex between pyrazoline and anthracene moieties of the two neighboring molecules was identified to emit at the wavelength of 540 nm, and the relative emission intensity increased as compared to that of the monomer with an increase in the particle diameters. Such an observation may present an alternate approach for achieving color modulation for electroluminescent (EL) materials. With the consideration of organic materials in the future luminescence applications, the size-tunable emission presented by DAP nanoparticles is likely to be important.

## Experimental Section

**Materials.** The model compound used in our work, 1,3-diphenyl-5-(2-anthryl)-2-pyrazoline (DAP, Scheme 1), was synthesized as described elsewhere.<sup>18</sup> The target product was purified using liquid chromatography, and its structure was confirmed by nuclear magnetic resonance (NMR) and mass spectroscopy (MS). Acetonitrile (for HPLC use) was used as the good solvent of DAP and was purchased from ACROS. Ultrapure water with a resistivity of 18.2 M $\Omega$  cm was produced using a Milli-Q apparatus (Millipore) and was filtered using an inorganic membrane with a pore size of 0.02  $\mu$ m (Whatman International, Ltd.) just before use.

**Methods.** The organic nanoparticles of DAP were prepared through the reprecipitation method.<sup>11,12,13,15</sup> In a typical preparation, 150  $\mu$ L of DAP–acetonitrile stock solution ( $2.0 \times 10^{-3}$  mol/L) was rapidly injected (<2 s) into 5 mL of water at room temperature (25  $^{\circ}$ C). Mixing of acetonitrile with the water phase rapidly changes the character of the solvent and induces nucleation and growth of DAP nanoparticles. The average particle size was controlled through a ripening process by the variation of the aging time, that is, by changing the time intervals after the stock solution injection. For example, the particles with an

average diameter of 40 and 160 nm were obtained when the system was aged for 4 and 36 h, respectively, at the ambient temperature of 25  $^{\circ}$ C.

The sizes and distributions of the nanoparticles dispersed in water were evaluated in situ by the dynamic light scattering (DLS) technique using a particle size analyzer (BI-90Plus, Brookhaven Instruments Corp., Holtsville, NY) with a scattering angle of 90 $^{\circ}$ . The surface electric  $\xi$ -potential measurement was conducted with palladium electrode assembly using the ZetaPALS (phase analysis light scattering) technique at a pH value of 6.50 at room temperature (25  $^{\circ}$ C). The sizes and shapes of the nanoparticles were observed on a field emission scanning electron microscope (FESEM, JSM-6700F, JEOL) at an accelerating voltage of 3 kV. To enhance the conductivity of the sample, a layer of platinum was sputtered at a current of 5 mA and a pressure of 3 mmHg. The samples were also characterized on a D/max-2400 X-ray diffractometer with an X-ray source of Cu/K- $\alpha$  at 40 kV and 120 mA after being filtered onto an inorganic membrane with pore size of 0.02  $\mu$ m (Whatman International, Ltd.). The samples were then transferred onto the copper grids for electron diffraction characterization by gently wiping with a tip. Electron diffraction patterning of the particles with different sizes was performed on the transmission electron microscope (JEM-200CX, JEOL) at an accelerating voltage of 200 kV.

The UV–visible absorption spectra and the steady-state excitation and emission fluorescence spectra of the aliquots of the DAP nanoparticle dispersion in water were measured in situ using a Shimadzu UV-1601 PC double-beam spectrophotometer and a Hitachi F-4500 fluorospectrometer, respectively. Time-resolved fluorescence measurements were carried out at the ambient temperature of 25  $^{\circ}$ C on a Horiba NAES-1100 time-resolved spectrofluorometer with a single-photon counting system. DLS and FESEM measurements showed that, during the above optical characterization, the average particle sizes and the size distributions do not change much.

The structure of one DAP molecule was drawn, and the minimum energy configuration was optimized by energy minimization using the B3LYP/6-31G method as implemented in Gaussian 98. Molecular modeling calculations of the structure of the two-DAP-molecule pair in the nanoparticles were conducted using the AM1 (Austin Model 1) semiempirical quantum mechanical method. The minimization procedure involves systematically changing the coordinates of the atoms and groups, and the conformation with a minimum energy of the system was reachable. The electronic excited state of the dimer was calculated by the method of single configuration interaction (SCI) using the ZINDO program and analyzed using ZOAV2 software. The modeling calculation was also done using a MMX force field in PCMODEL6.0 developed by Serena Software, Bloomington, IN, which is suitable for the modeling calculation of the Pi-molecular system.

## Results and Discussion

A series of DAP nanoparticles with different average sizes in diameter from 40 to 160 nm were successfully prepared in our experiment by controlling the aging time. The DAP nanoparticle aqueous dispersion exhibits the characteristic Tyndall effect as did those of inorganic colloidal systems. Figure 1 displays some field emission scanning electron microscope images of the as-prepared DAP nanoparticles, in which the average sizes were 60 nm (A) and 160 nm (B), respectively. DLS evaluation of the aliquots indicated that the size distributions of the particles are very narrow. The polydispersities of the samples are less than 0.1 (10%). Measurements of surface electric properties indicate that these nanoparticles are all negatively charged, and their  $\xi$ -potentials retain a value of ca. –28 mV for all of the nanoparticles with different sizes at a pH value of 6.50. This kind of surface electric feature may originate from the selective adsorption<sup>22</sup> of the OH $^{-}$  anion,

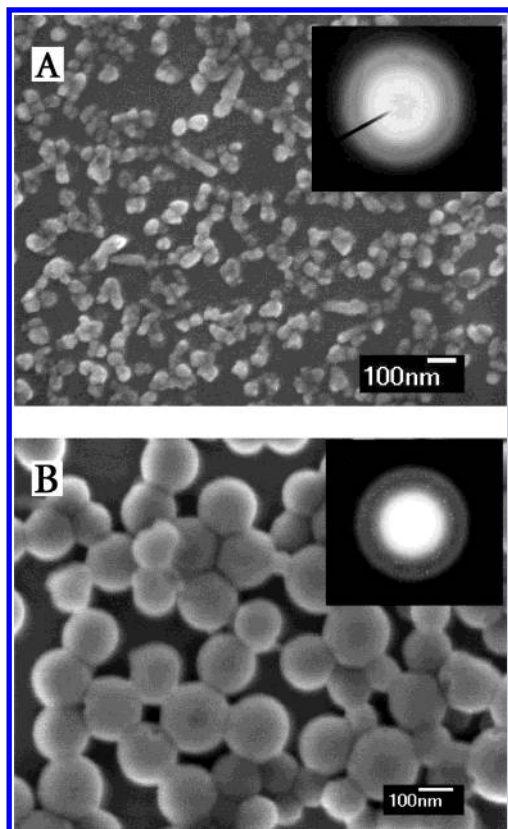


**Figure 1.** Field emission SEM images of DAP nanoparticles with average diameters of (A) 60 nm and (B) 160 nm. The insets are electron diffraction patterns of the corresponding particles.

which came from the ionization of water. XRD measurement presented no characteristic diffraction peaks for the samples with different diameters, and electron diffraction patterns with two halos of the same samples with diameters of 60 and 160 nm are displayed in the insets of Figure 1. These results confirm that the particles are unambiguously amorphous. Such an amorphous character of DAP nanoparticles should be profitable to the light-emitting efficiency because of the reduction in quenching from the internal conversion process which is dominant in the crystalline systems.<sup>1</sup>

Figure 2 shows the UV–visible absorption spectra of DAP nanoparticle dispersions in water with different sizes (lines a–e) and in DAP/acetonitrile dilute solution (line s). In the case of the solution, the spectrum exhibits a vibronically structured band in the 330–410 nm region, which is attributed to a superposition of absorption transitions of anthracene ( $1A_{1g} \rightarrow 1B_{2u}$ )<sup>23</sup> and the pyrazoline ring,<sup>15,21,24</sup> and a higher-energy band at 254 nm ( $1A_{1g} \rightarrow 1B_{3u}$ , anthracene)<sup>23</sup>. The absorption of DAP nanoparticles was substantially different from that of the solution, and the evolution of absorption was studied as a function of particle size. In the spectra of DAP nanoparticles, the low-energy absorption band centered at 365 nm in the 330–410 nm region experiences a slight bathochromic shift with an increase in the particle sizes. Simultaneously, the high-energy band of anthracene was split, which is ascribed to the electronic coupling between the neighboring molecules in the particles.<sup>25</sup> In addition,

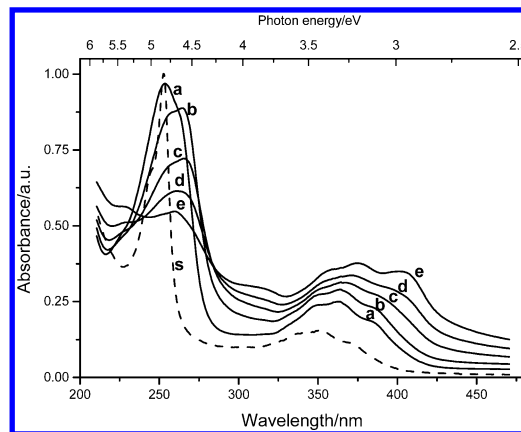


**Figure 2.** Absorption spectra of DAP nanoparticle dispersions with different sizes and DAP solution in acetonitrile. Line s, the spectrum of DAP solution; a, 40 nm; b, 60 nm; c, 90 nm; d, 120 nm; e, 160 nm.

the trailing edge of the spectra at long wavelengths became more pronounced for the larger particles than for the smaller ones due to Mie scattering effects.<sup>26</sup>

As far as the absorption transition of DAP nanoparticles is concerned, the bathochromic shift of the low-energy region is expected to be similar to the previous observations of absorption by aggregate states in other organic molecular crystals such as  $\alpha$ -perylene<sup>27</sup> and tetracene.<sup>28</sup> This leads us to assign it to the effect similar to the red shift with an increase in the size of the molecular aggregates. The size of regions of local order may increase as the nanoparticle size increases, allowing the intermolecular electronic interactions to increase in magnitude and to extend over a larger number of molecules. It is known that the split band in the high-energy side was observed in the mixed dimer<sup>23,25,29</sup> of different substituted anthracenes, which is attributable to the coupling of the electronic transitions. The spatial configuration of two DAP molecules with the minimum potential energy in the nanoparticles was optimized via the AM1 semiempirical quantum mechanical calculation (a similar result is reachable by the MMX force field molecular modeling calculation, please see Supporting Information), as shown in Figure 3. It is demonstrated that the anthracene group of one molecule and the pyrazoline ring of the neighboring one are in a face-to-face stacking mode. This interlaced arrangement of anthracene and pyrazoline groups in two adjacent molecules lends support to the possibility of the electronic coupling between these two chromophores. Thus, we proposed that the splitting of the higher-energy band in the absorption spectra originates from the electronic coupling between the pyrazoline ring of one molecule and the anthracene moiety of the neighboring molecule. The existence of such an effect is also supported by the gradual predominance of the absorption transition of the pyrazoline group, in which the relative intensities of the electronic bands within the molecules are changed.

Figure 4 shows fluorescence excitation spectra of DAP nanoparticle dispersions in water with different sizes (lines a–e).

(22) Leja, J. *Surface Chemistry of Froth Flotation*; Plenum Press: New York, 1982.

(23) Chandross, E. A.; Ferguson, J. *J. Chem. Phys.* **1966**, *45*, 3554.

(24) Wilkinson, F.; Kelly, G. P.; Michael, C. J. *Photochem. Photobiol. A: Chem.* **1990**, *52*, 309–320.

(25) Chandross, E. A.; Ferguson, J.; McRae, E. G. *J. Chem. Phys.* **1966**, *45*, 3546.

(26) Auweter, H.; Habernorn, H.; Hechmann, W.; Horn, D.; Luddecke, E.; Rieger, J.; Weiss, H. *Angew. Chem., Int. Ed.* **1999**, *38*, 2188–2191.

(27) Tanka, J. *Bull. Chem. Soc. Jpn.* **1963**, *36*, 1237.

(28) Kelly, M. K.; Etchegoin, P.; Fuchs, D.; Kratschmer, W.; Fostiropoulos, K. *Phys. Rev. B* **1992**, *46*, 4963.

(29) Sidman, J. W. *J. Chem. Phys.* **1956**, *25*, 115.

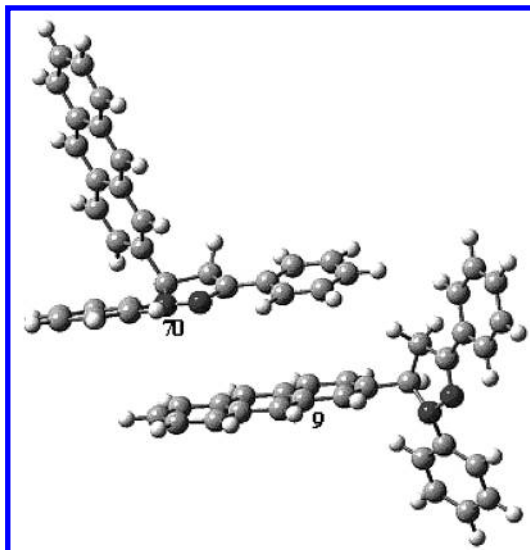


**Figure 3.** Optimized stacking mode of two DAP molecules in nanoparticles using the AM1 semiempirical quantum mechanical method.

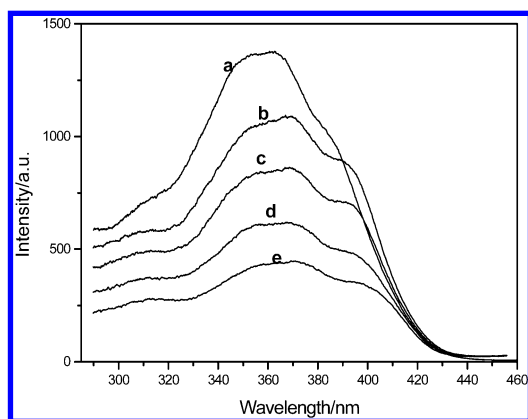


**Figure 4.** Fluorescence excitation spectra of DAP nanoparticle dispersions with different sizes and DAP solution in acetonitrile. Line a, 40 nm; b, 60 nm; c, 90 nm; d, 120 nm; e, 160 nm. The emission wavelength is at 540 nm.

The emission is monitored at the wavelength of 540 nm. One can see that the prominent feature of the excitation spectra of the particles is the change in the wavelength region similar to those in the absorption spectra. As the particle size increases, the excitation spectra in the 300–440 nm region also experience a slight bathochromic shift. Similar results were obtained when the excitation spectra were recorded at the emission wavelength of the pyrazoline chromophore in the region of 440–490 nm, except for the fact that the emission intensities were all higher than those at 540 nm.

The evolution of emission from the DAP nanoparticles was investigated as a function of particle size, as shown in Figure 5, in which all of the spectra were normalized by the maximum emission of line a. The emission spectrum of the molecularly dispersed DAP in acetonitrile (line s) shows the only characteristics of the anthracene group<sup>23</sup> of the monomeric emission at 370–500 nm. The absence of pyrazoline emission is due to the solvent quenching of the twisted intramolecular charge transfer from N-1 to C-3.<sup>24,30</sup> There are significant differences between the fluorescence of the DAP nanoparticles and that of

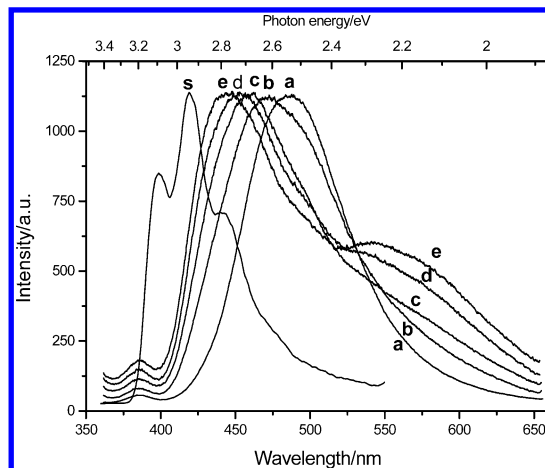


**Figure 5.** Fluorescence emission spectra of DAP nanoparticle dispersions with different sizes and DAP solution in acetonitrile. Line s, the spectrum of DAP solution; a, 40 nm; b, 60 nm; c, 90 nm; d, 120 nm; e, 160 nm. The excitation wavelength is at 350 nm.

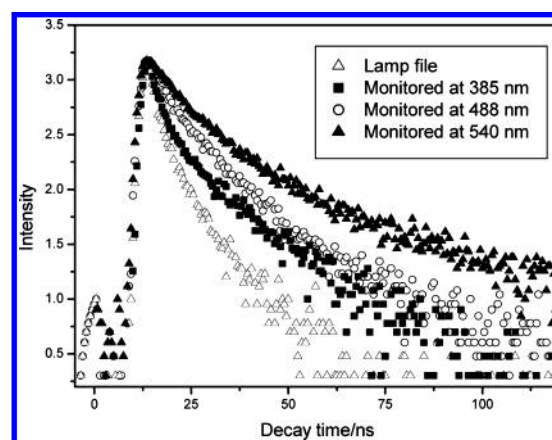


**Figure 6.** Fluorescence decay profiles of 40 nm DAP nanoparticles monitored at 385 nm (■), 488 nm (○), and 540 nm (▲).

the monomers. The nanoparticles with a size of 40 nm show the emission of anthracene (385 nm)<sup>23</sup> and the pyrazoline group at 488 nm,<sup>24</sup> shown as line a. With an increase in the particle size, the emission of the pyrazoline group experiences a hypsochromic shift by a maximum of 45 nm, appearing at 443 nm when the particle size is 160 nm. At the same time, a new broad and structureless emission feature centered at 540 nm emerges and becomes gradually prominent with particle growth. Moreover, the emission from anthracene is slightly intensified with the growth of the particles. No evident changes in the shape of the solution and the nanoparticles emission spectra are observed as the excitation wavelength changes from 254 to 355 nm.

The fluorescence lifetimes of the nanoparticle suspensions with different sizes were measured with an excitation light of 350 nm to further understand the nature of the excited state. It is shown that the lifetimes of the excited state of the nanoparticles also show size-dependent behaviors. The fluorescence decay profiles of the nanoparticle dispersion with 40 nm were monitored at 385, 490, and 540 nm, as shown in Figure 6. The lifetime of anthracene emission (monitored at 385 nm) is prolonged from 1.50 to 2.32 ns with the growth of the particles from 40 to 160 nm. The emission decay profiles monitored in the region of 440–490 nm can be well fitted to be dual-

(30) (a) Morley, J. O.; Docherty, V. J.; Pugh, D. *J. Mol. Electron.* **1989**, *5*, 117.  
(b) Yan, Z. L.; Hu, G. W.; Wu, S. K. *Acta Chim. Sin.* **1995**, *53*, 227.

**Table 1.** Atomic Charge of the Related Atoms before and after the Charge-Transfer Process<sup>a</sup>

atom number	atom type	atomic charge before CT	atomic charge after CT
70	N	-0.597892	-0.1871
9	C	0.077297	-0.0398

<sup>a</sup> The calculated electronic state is the ninth excited state.

exponential. For example, the decay curve of the 40 nm nanoparticles monitored at 488 nm is resolved into two components with high accuracy, a short lifetime of 3.57 ns (84.6%) and a long component of 17.2 ns (15.4%). Those monitored at 540 nm were determined to have two components, the short one  $\tau_{1,540} = 6.39 \pm 0.112$  ns (52.3%), and the other long component  $\tau_{2,540} = 20.2 \pm 0.430$  ns (47.7%). For the 160 nm particles monitored at 443 nm, the two lifetime values are 2.58 ns (52.8%) and 12.4 ns (47.2%), respectively. The lifetime monitored at 540 nm decreased to  $\tau_{1,540} = 5.78 \pm 0.0842$  ns (57.1%) and  $\tau_{2,540} = 18.8 \pm 0.479$  ns (42.9%).

In the emission spectrum of the solution, the characteristic feature of pyrazoline arising from the intramolecular charge-transfer process was quenched due to the solvent effect. However, this feature of pyrazoline emission appeared in the nanoparticles, and the vibrational structure of anthracene disappeared. In terms of the emission for large particles at 540 nm, the broad and structureless structure exhibiting a dual-exponential decay curve with a long lifetime component as compared to that of the pyrazoline chromophore is indicative of the existence of the complex in the nanoparticles. In fact, the face-to-face packing as shown in Figure 3 facilitates the dimer to form the complex. In organic molecules, the complex state generally exhibits a long decay time as compared to that of the initially excited state.<sup>31</sup> The long lifetime components monitored at 488 and 443 nm also confirm the existence of the complex state, while the one with short lifetime was assigned to the emission from the pyrazoline chromophore.<sup>24,30</sup> The above spectral feature accompanying the absorption and excitation spectra similar to the former ones leads us to conclude that there exists a complex in DAP nanoparticles and the complex is an exciplex, that is, the excited-state complex. This is in accordance with the absence of absorption character in the longer wavelength region (410–450 nm), which emerged in PDDP and DPP nanoparticles as we reported previously.<sup>13,15</sup> It is known that the exciplex possesses the characteristic of charge transfer.<sup>32,33</sup> This feature of the dimer in DAP nanoparticles is also supported by the quantum mechanics calculation. The single configuration interaction result of the quantum calculation demonstrated that there exists a charge-transfer process between atom 70 (N1 atom in the one molecule) and atom 9 (one carbon atom in another molecule) in the excited state, as shown in Table 1.

It is obvious that the spectral evolution is the result of particle growth. It deserves mentioning that such a size-dependent optical property of DAP nanoparticles cannot be attributed to the confinement effect because the radii of Frenkel and CT excitons in organic materials are so small<sup>1</sup> that the quantum size effect should be negligible for particles larger than 10 nm in diameter.

The size-tunable absorption and emission exhibited by organic nanoparticles of DAP are also unlikely to originate from the Mie scattering, which is often found in metal nanocrystals. In fact, the peak broadening with an increase in the particles cannot be elucidated in terms of Mie scattering. To explain the similar size dependence of organic nanoparticles such as perylene, Nakanishi proposed two possible reasons.<sup>3,4</sup> One is the change of lattice state due to the increase in surface area. It is likely that the increase in surface area causes lattice softening, and then the Coulombic interaction energies become smaller, leading to wider band gaps. The other reason may be the electric field effect of the surrounding environment through the surface of the particles. The fact that the nanoparticles with different sizes bear almost the same  $\xi$ -potential indicates that this may not be the main factor responsible for the optical size-tunability of DAP nanoparticles.

From Figure 3, we can see that the anthracene ring in one molecule and pyrazoline chromophore in the other overlap to some extent. As the nanoparticle size increased, the enhanced intermolecular interaction<sup>3,4,5,7</sup> also enhanced the degree of the chromophores' overlap, and the increased dipole–dipole interaction led to a narrow band gap, resulting in the absorption shifting to the lower-energy side. Note that the gradual dominance of the pyrazoline absorption feature and the splitting of the  $^1A_{1g} - ^1B_{3u}$  transition of anthracene with an increase in the particle size indicate that the electronic coupling between the molecules occurred and increased with the growth of the particles. Therefore, the split band became pronounced with an increase in the particle size. With an increase in the particle size, the enhanced interaction between the molecules led to the pronounced decrease in the Stokes shift (the shift between the maxima of the fluorescence and absorption) because they restrain the vibronic relaxation and the configuration reorganization of the excited states. The calculated Stokes shift of 0.866 eV for the 40 nm particles decreased, via 0.626 eV for the particles of 90 nm, to 0.501 eV for the 160 nm particles. Such an evolution of Stokes shift ( $W_s$ ) is similar to that identified for disordered molecular aggregates<sup>34</sup> in which  $W_s$  decreases monotonically with the aggregate size. Thus, the blue-shifted pyrazoline emission originates from the reduction in Stokes shift, which is caused by the increased intermolecular interaction with an increase in the particle size.

At the same time, with the growth of the nanoparticles, the orientation between the two moieties was adjusted to be beneficial to the formation of exciplex, leading to the intensified emission from the exciplex in the nanoparticles with an increase in the particle size. Therefore, the size-tunability of absorption and emission exhibited by DAP nanoparticles is due to the increased intermolecular interaction.

## Conclusion

In summary, amorphous DAP nanoparticles with a range of average diameters from 40 to 160 nm were prepared through the reprecipitation method. We found that DAP nanoparticles exhibit the size-dependent bathochromic absorption transition and the split band of the higher-energy band of anthracene. The hypsochromically shifted emission of the pyrazoline chromophore was observed in the blue light region with an increase

(31) Fox, M. A.; Chanon, M. *Photoinduced Electron Transfer, Part A*; Elsevier: New York, 1988.

(32) Gordon, M.; Ware, W. R. *The Exciplex*; Academic Press, Inc.: New York, 1975.

(33) Kuchitsu, K. *Dynamics of Excited Molecules*; Elsevier: New York, 1994.

(34) Chernyak, V.; Meier, T.; Tsiper, E.; Mukamel, S. *J. Phys. Chem. A* **1999**, *103*, 10294–10299.

in the particle size due to the restraint of the vibronic relaxation and the configuration reorganization process of the electronically excited state. An exciplex between pyrazoline and anthracene moieties of the two neighboring molecules was identified to emit green light at the wavelength of 540 nm. The emission intensity from the exciplex increased as compared to that of the monomer with the growth of the nanoparticles. Such an evolution of the optical properties of the organic nanoparticles as a function of particle size presents us with another strategy to tune the color of the light emitted for electroluminescent materials only by the variation of the particle size. It is likely to play a vital role in the fabrication of novel optoelectronic devices in the future.

**Acknowledgment.** The authors would like to express their sincere thanks for the support of the National Science Founda-

tion of China, the Chinese Academy of Sciences, and the National Research Fund for Fundamental Key Projects No. 973 (G19990330). The authors also thank the reviewers for providing numerous helpful suggestions for revising this manuscript.

**Supporting Information Available:** Optimized structure of a two-DAP-molecule pair by the MMX molecular force field, which is in accordance with that optimized by the AM1 method, showing the atom numbers, and the exciton state with charge transfer between the two molecules analyzed using ZOAV2 software (PDF). This material is available free of charge via the Internet at <http://pubs.acs.org>.

JA028674S